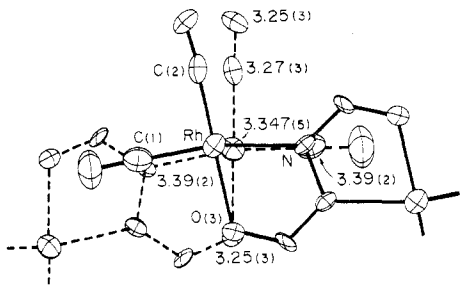

Figure 2. A view of the interaction between an adjacent pair of dimers. Close contact distances corresponding to those for symmetry transformation I in Table IV are shown. An equivalent interaction with a molecule above the plane of the paper involves Rh′ and is generated by the molecular center of symmetry. In this way, the one-dimensional chain is propagated in a "stepwise" fashion with Rh atoms interacting in pairs.

and unrelated to the molecular stacking. The stacked molecules are related by transformation I (a twofold axis) with a Rh–Rh distance of 3.347 (5) Å. This separation is longer than expected for a Rh–Rh single bond but of a magnitude comparable to that of 3.31 Å for the intermolecular Rh–Rh contact in $[Rh(CO)_2Cl]$.[2] Contacts of this magnitude have commonly been associated with weak metal–metal interactions. It is interesting to note that the displacement of the metal atom from the OCNNCO plane is such that the Rh atoms involved in the 3.347 Å separation are displaced toward each other from their respective ligand planes.

The one-dimensional chain formed by these short intermolecular interactions is propagated in a "stepwise" rather than a linear fashion. This is readily apparent from Figure 2 if one recalls that there is a center of symmetry at the midpoint of each N–N bond. Thus the dimer (not shown) above the plane of the paper would have a short metal–metal contact to the rhodium atom at the extreme right of the figure. In principle, there is a pathway for electron delocalization along this chain via the short metal–metal separations and a delocalized π pathway through the bridging ligands. However, this would not be expected to be a large effect because of the length of the Rh–Rh contacts and the apparent lack of extensive delocalization through the N–N bonds. The very small size of the crystals obtained to date precludes any attempt to measure anisotropic conductance properties.

Chemical and spectroscopic evidence indicates that a similar bridging configuration is adopted by the dibenzoylhydrazido ligand in the entire reported series of binuclear Rh(I) and Ir(I) complexes of this ligand.[7] Although these are the first compounds in which this ligand bridges in a bis bidentate fashion, it is evident that the bridging system is a very stable one, since it remains intact through both substitution and oxidation reactions at the metal ion. This bridging group offers potential π pathways for metal–metal interaction; hence it would be of interest to investigate its complexes with paramagnetic metal ions.

Registry No. $[(CO)_2RhN(COPh)]_2$, 59671-04-4.

Supplementary Material Available: Table A, a listing of structure factor amplitudes, and Table B, a tabulation of principal amplitudes of thermal motion (7 pages). Ordering information is given on any current masthead page.

References and Notes

(1) F. M. Hussein and A. S. Kasenally, *J. Chem. Soc., Chem. Commun.*, 3 (1972).
(2) L. F. Dahl, C. Martell, and D. L. Wampler, *J. Am. Chem. Soc.*, **83**, 1761 (1961).
(3) R. J. Doedens and J. A. Ibers, *Inorg. Chem.*, **8**, 2709 (1969).
(4) R. J. Doedens, *Inorg. Chem.*, **9**, 429 (1970).
(5) R. G. Little and R. J. Doedens, *Inorg. Chem.*, **11**, 1392 (1972).
(6) S. D. Ittel and J. A. Ibers, *Inorg. Chem.*, **12**, 2290 (1973).
(7) A. S. Kasenally and F. M. Hussein, *J. Organomet. Chem.*, **111**, 355 (1976).
(8) Computer programs employed in this work have previously been listed by R. G. Little and R. J. Doedens, *Inorg. Chem.*, **12**, 844 (1973).
(9) P. W. R. Corfield, R. J. Doedens, and J. A. Ibers, *Inorg. Chem.*, **6**, 197 (1967); R. J. Doedens and J. A. Ibers, *ibid.*, **6**, 204 (1967).
(10) Nonstandard setting of No. 15, $C2/c$. Equivalent positions: (0, 0, 0; $^1/_2$, $^1/_2$, $^1/_2$) ± (x, y, z; $^1/_2 - x$, y, $\bar{z}$).
(11) "International Tables for X-Ray Crystallography," Vol. 4, Kynoch Press, Birmingham, England, 1974.
(12) Supplementary material.
(13) J. A. Evans and D. R. Russell, *Chem. Commun.*, 197 (1971).
(14) J. Ječný and K. Huml, *Acta Crystallogr., Sect. B*, **30**, 1105 (1974).
(15) D. Allen, C. J. L. Lock, G. Turner, and J. Powell, *Can. J. Chem.*, **53**, 2707 (1975).
(16) A. C. Jarvis, R. D. W. Kemmitt, B. Y. Kimura, D. R. Russell, and P. A. Tucker, *J. Chem. Soc., Chem. Commun.*, 797 (1974).
(17) S. W. Kaiser, R. B. Saillant, W. M. Butler, and P. G. Rasmussen, *Inorg. Chem.*, **15**, 2681, 2688 (1976).
(18) L. G. Kuzmina, Yu. S. Varshavskii, N. G. Bokii, Yu, T. Struchkov, and T. G. Cherkasova, *J. Struct. Chem. (Engl. Transl.)*, **12**, 593 (1971).
(19) L. Pauling, "The Nature of the Chemical Bond", 3rd ed, Cornell University Press, Ithaca, N.Y., 1960, Chapter 7.
(20) R. J. Baker, S. C. Nyburg, and J. T. Szymanski, *Inorg. Chem.*, **10**, 139 (1971).

Contribution from Materials and Molecular Research Division, Lawrence Berkeley Laboratory, and the Department of Chemistry, University of California, Berkeley, California 94720

Crystal Structure of $XeF^+AsF_6^-$[1]

ALLAN ZALKIN, DONALD L. WARD, RICHARD N. BIAGIONI, DAVID H. TEMPLETON,* and NEIL BARTLETT*

Received October 26, 1977

Crystals of $XeF^+AsF_6^-$ are monoclinic, space group $P2_1/n$, a = 6.308 (3) Å, b = 6.275 (3) Å, c = 16.023 (5) Å, β = 99.97 (5)°, V = 624.66 Å^3, Z = 4, and d_x = 3.61 g cm^{-3}, at 24 °C. X-ray diffraction data were measured with counter methods and Mo Kα radiation. With anisotropic temperature factors for all atoms, R = 0.033 for 777 independent reflections ($I > 3\sigma$). The structure consists of ion pairs connected by a bridging fluorine atom into $FXeFAsF_5$ units. The FXeF portion of the molecule is linear (angle = 178.9 (7)°) with Xe–F = 1.873 (6) Å (terminal) and 2.212 (5) Å (bridging). The $FAsF_5$ portion of the molecule is roughly octahedral with cis F–As–F angles ranging from 85.3 (3) to 94.6 (5)°; the five terminal As–F distances range from 1.676 (5) to 1.690 (8) Å and the bridging As–F distance is 1.813 (6) Å. The bridge Xe–F–As angle is 134.8 (2)°.

Introduction

In an earlier paper Sladky et al. described[2] the preparation of the 1:1 XeF_2–AsF_5 complex and showed that it lost AsF_5 readily under vacuum at ordinary temperatures to yield a 2:1 complex. The crystal structure of the 2:1 complex has already been described[3] and is consistent with formulation as the salt $Xe_2F_3^+AsF_6^-$. The structure of the 1:1 complex was of interest to us because of an earlier finding[4] that the structure of the 1:1 XeF_2–RuF_5 complex was consistent with the $XeF^+RuF_6^-$ formulation and our expectation that the formulation of the 1:1 XeF_2–AsF_5 complex would be similar. Moreover, a preliminary study of 1:1 XeF_2–AsF_5 by others[5] had failed to

0020-1669/78/1317-1318$01.00/0 © 1978 American Chemical Society

Table I. X-Ray Powder Data for $XeF^+AsF_6^-$ (from a Sample in 0.3 mm Diameter Quartz Capillary Using Cu Kα Radiation)

	Calcd		Obsd	
hkl	$1/d^2$	$pF^2/10^4$	$1/d^2$	Intensity
002	0.0161	3	0.0170	vw
$11\bar{1}$	0.0518	232	0.0515	s
111	0.0588	177	0.0586	s
004	0.0642	156	0.0648	s
?			0.0706	vvw
112	0.0744	14	0.0774	m
$11\bar{3}$	0.0768	76		
014	0.0896	6	0.0885	vw
113	0.0980	105		
020	0.1016	137	0.0988	mw
200	0.1036	147		
021	0.1056	23		
$20\bar{2}$	0.1056	5	0.1080	m
$10\bar{5}$	0.1086	6		
120	0.1275	11	0.1241	w
$12\bar{1}$	0.1280	9		
$11\bar{5}$	0.1340	70	0.1347	w
121	0.1350	11		
$20\bar{4}$	0.1396	82		
006	0.1445	18	0.1396	w
105	0.1440	7		
023	0.1377	11		
212	0.1592	70	0.1599	w
024	0.1658	123	0.1679	w
115	0.1693	98		
204	0.1961	65	0.1970	w
$10\bar{7}$	0.1979	10		
220	0.2052	65		
$20\bar{6}$	0.2058	11	0.2059	w
124	0.2059	4		
$12\bar{5}$	0.2102	13		
$21\bar{6}$	0.2312	37	0.2349	w
$22\bar{4}$	0.2412	74	0.2426	w
008	0.2570	80		
$31\bar{1}$	0.2520	101	0.2550	mw
$13\bar{1}$	0.2549	70		
131	0.2620	47	0.2635	mw
$31\bar{3}$	0.2629	27		
224	0.2977	59	0.3019	w
027	0.2983	16		
$31\bar{5}$	0.3059	135		
$20\bar{8}$	0.3041	48	0.3077	w
133	0.3012	40		
$11\bar{9}$	0.3447	87	0.3484	vw
119	0.4083	108		
208	0.4171	44		
400	0.4145	56	0.4090	w
040	0.4062	34		
0,0,10	0.4015	18		

find evidence of AsF_6^- and the authors concluded that this indicated that the complex was a molecular, possibly fluorine-bridged, adduct.

We give here the preparative conditions for 1:1 XeF_2–AsF_5 complex and the structure determined by single-crystal x-ray diffraction.

Experimental Section

Preparation of $XeFAsF_6$. XeF_2 (0.684 g, 4.04 mmol), prepared as described by Williamson,[6] was transferred in the dry nitrogen atmosphere of a Vacuum Atmospheres Corp. Drilab to a weighed quartz bulb (~60 cm³ capacity) joined to a Brass Whitey valve (IKS4) with a Teflon-gasketed Swagelock fitting. Bromine pentafluoride (Matheson Co., East Rutherford, N.J.) sufficient (~2 mL) to dissolve the XeF_2 was transferred to the bulb under vacuum. The resultant, almost colorless solution of XeF_2 in BrF_5 was exposed to arsenic pentafluoride gas (Ozark Mahoning, Tulsa, Okla.) to maintain a pressure of ~900 Torr. A small Teflon-coated stirrer bar driven by an external magnet kept the solution mixed. The solution rapidly became pale yellow-green but the system was left for ~1 h to ensure full takeup of AsF_5 gas. The solution was cooled to −22.8 °C (CCl_4 slush) and the bulk of the BrF_5 was removed in a dynamic vacuum. (At the beginning of this evaporation the valve was opened slowly to ensure smooth boiling and to avoid frothing.) The crystalline solid so obtained was dried by intermittent opening and closing of the valve, for a few minutes, with the sample at room temperature. The solid remaining in the trap was almost white, with a pale yellow-green tint. It amounted to 1.372 g, indicating an AsF_5 uptake of 0.688 g (4.05 mmol) which corresponds to a XeF_2:AsF_5 molar ratio of 1:1.002.

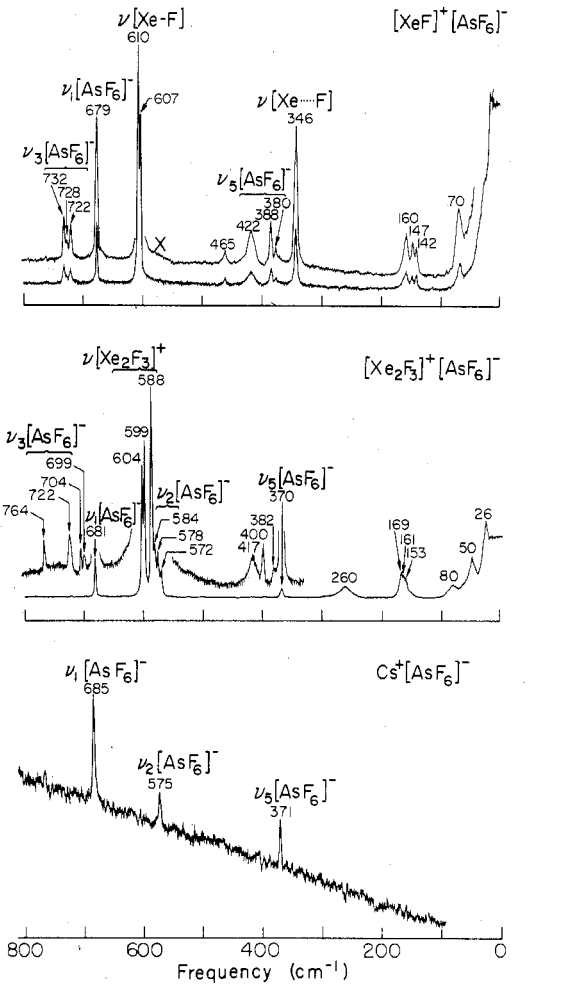

Figure 1. The spectra of $XeFAsF_6$ and $Xe_2F_3AsF_6$ are seen to be similar and the counterparts of the ν_1 and ν_5 modes are seen, from comparison with the $CsAsF_6$ spectrum, to be present in both. $Xe_2F_3AsF_6$ consists of well-separated ions $Xe_2F_3^+$ and AsF_6^- (ref 3) whereas in $XeFAsF_6$ there is a unique interaction of cation and anion. This interaction is probably responsible for the relatively intense band at 346 cm^{-1} in $XeFAsF_6$. Similar assignments, but with a different bonding interpretation, have been given by Gillespie and Landa (*Inorg. Chem.*, **12**, 1385 (1973)); our spectrum of $XeFAsF_6$ shows less $Xe_2F_3AsF_6$ impurity (×) than theirs and fine structure and weak bands previously unrecorded.

X-ray powder photographs were obtained by rapidly transferring the solid to a 0.5-mm quartz x-ray capillary in the Drilab. The capillary was sealed with a small flame. The data given in Table I were indexed using the single-crystal information.

Single crystals of $XeFAsF_6$ were grown by sublimation of small samples of the powder sealed, as in the x-ray powder sample case, under nitrogen in thin-walled quartz x-ray capillaries. These capillaries were placed in an electrically heated tube which provided for a temperature gradient along the capillary of 1 or 2 °C at a temperature of ~70 °C. The capillaries were left in this heater overnight and were then inspected for single-crystal development using a polarizing microscope.

Raman spectra were obtained from a sample packed as for the x-ray powder sample but in a 1.5 mm diameter quartz capillary. The sample was cooled by a cold nitrogen stream shrouded by a dry room temperature stream and the temperature was thereby maintained at ~−100 °C. The spectrum of $Xe_2F_3AsF_6$ was obtained in the same way. The spectra are compared in Figure 1.

Table II. Coordinates and Thermal Parameters for $XeF^+AsF_6^-$ [a]

	x	y	z	B_{11}	B_{22}	B_{33}	B_{12}	B_{13}	B_{23}
Xe	0.25918 (9)	0.21684 (12)	0.62266 (3)	3.94 (3)	4.32 (3)	3.51 (2)	−0.46 (3)	0.67 (2)	0.07 (2)
As	0.23792 (13)	0.27638 (18)	0.39041 (5)	3.32 (4)	3.83 (5)	3.56 (3)	−0.19 (4)	0.46 (3)	−0.21 (3)
F(1)	0.4950 (8)	0.2815 (14)	0.3763 (4)	4.4 (3)	9.4 (5)	8.1 (4)	−0.6 (3)	2.4 (3)	0.0 (3)
F(2)	0.2308 (13)	0.5447 (14)	0.3816 (5)	8.6 (5)	4.8 (4)	11.8 (6)	0.5 (4)	2.6 (4)	1.1 (3)
F(3)	0.1413 (12)	0.2335 (16)	0.2889 (4)	8.9 (4)	15.2 (8)	3.9 (3)	−3.3 (5)	0.1 (3)	−1.8 (4)
F(4)	−0.0092 (9)	0.2721 (13)	0.4177 (5)	4.0 (3)	8.7 (5)	8.7 (4)	−0.2 (3)	2.1 (3)	−0.2 (3)
F(5)	0.2512 (14)	0.0141 (13)	0.4127 (6)	9.1 (5)	4.1 (4)	13.9 (6)	0.2 (4)	1.6 (4)	0.9 (4)
F(6)	0.3466 (12)	0.3220 (15)	0.5013 (3)	7.1 (3)	13.1 (6)	3.8 (2)	−5.4 (5)	0.1 (2)	0.5 (2)
F(7)	0.1843 (13)	0.1334 (19)	0.7260 (4)	11.2 (6)	15.5 (7)	4.8 (3)	−5.2 (5)	3.0 (3)	1.3 (4)

[a] Estimated standard deviation of the least significant digit(s) is given in parentheses here and in the following tables. The form of the temperature factor is $\exp[-0.25(h^2a^{*2}B_{11} + 2hka^*b^*B_{12} + \ldots)]$. For space group $P2_1/n$ (an alternate setting of $P2_1/c$) the general positions are $x, y, z; -x, -y, -z; {}^1/_2 + x, {}^1/_2 - y, {}^1/_2 + z$; and ${}^1/_2 - x, {}^1/_2 + y, {}^1/_2 - z$.

X-Ray Measurements. The crystal selected for diffraction measurements was 0.09 × 0.11 × 0.15 mm in size. Precession photographs established the lattice to be monoclinic. Absent reflections $h0l$ ($h + l \neq 2n$) and $0k0$ ($k \neq 2n$) indicate space group $P2_1/n$. Setting angles for the Picker FACS-I diffractometer for 12 reflections above $2\theta = 45°$ (λ 0.709 26 Å for Mo $K\alpha_1$) were used for least-squares adjustment of the cell dimensions. Intensities were measured with graphite-monochromatized Mo $K\alpha$ radiation and θ–2θ technique for all reflections in the half-sphere with k nonnegative and $2\theta < 55°$. After averaging equivalent pairs there were 1447 unique data of which 783 had $I > 3\sigma(I)$. Measurements were made with a scan rate of 1°/min, backgrounds counted for 10 s each at an offset of 1° from each end of the scan, and a scan length of 1.5° in 2θ plus the α_1 – α_2 divergence. Three standard reflections showed slight irregular changes during the experiment, and a compensating correction (ranging from 1.00 to 1.10) was applied to the intensities. Correction for absorption[7] (μ = 103.4 cm^{-1}) was made by analytical integration with the crystal shape described by eight faces; factors ranged from 2.32 to 3.47. During refinement, effects of extinction became evident in the data, and an empirical isotropic correction was applied which increased the structure factors by 84 and 36% for the strongest and seventh-strongest reflections, respectively. The six strongest reflections were assigned zero weight because they failed to give good agreement even with this correction. A term $(0.03I)^2$ was added to the variance of I derived from counting statistics. Zero weight was also assigned to reflections with $I < 3\sigma$. Atomic scattering factors of Doyle and Turner[8] with anomalous scattering corrections of Cromer and Liberman[9] were used for neutral Xe, As, and F.

Crystal Data. $XeFAsF_6$: monoclinic, $P2_1/n$, a = 6.308 (3) Å, b = 6.275 (3) Å, c = 16.023 (5) Å, β = 99.97 (5)°, V = 624.66 Å^3, Z = 4, d_x = 3.61 g cm^{-3}, at 24 °C.

Determination of Structure. Analysis of a Patterson map indicated two sets of heavy atoms in general positions, a result incompatible with the preconceived opinion of the composition of the material.[10] For this reason the subsequent analysis was carried out using the diffraction data to establish the composition. The peaks for the heavy atoms were of appropriate relative height to correspond to Xe and As, and other peaks were found which corresponded to six F atoms around the As atom. Fourier maps phased with these eight atoms revealed the seventh fluorine atom. Another smaller peak was tested as a possible fluorine atom, but it was rejected by the least-squares refinement. A later electron density map, prior to the absorption correction and with $R = \sum|\Delta F|/\sum F_o = 0.10$, showed no other peaks as high as one-third the height of the lowest fluorine atom peak. The final refinement by full-matrix least squares reduced $R_w = [\sum w \cdot (\Delta F)^2/\sum wF_o^2]^{1/2}$, the quantity minimized, to 0.036. The final R was 0.033 for 777 reflections and 0.076 for 1447 reflections including those of zero weight. In the last cycle no parameter shifted more than 0.01σ. The goodness-of-fit was 1.13. Final parameters are listed in Table II.

Discussion

The crystal structure, Figure 2a, consists of an ordered arrangement of discrete $FXeFAsF_5$ units (Figure 3), the closest contact between units being 2.92 Å, a contact between F(1) and F(7). Bond distances and angles of this unit are listed in Tables III and IV. The amplitudes of thermal motion are considerable, and distances corrected for this motion according to the riding model are also listed in Table III. Table V gives the angles between principal axes of thermal motion of fluorine atoms and their bond vectors. In each case except Xe–F(6) the minimum amplitude of motion is nearly parallel to the bond, and in every case the largest amplitude is nearly perpendicular to the bond. These results lend credibility to the physical reality of this model of the thermal motion and support the propriety of the riding model. It may be noted that the consistency of As–F bond lengths (omitting the bridging bond which is not expected to be the same) is improved by the thermal correction.

Table III. Interatomic Distances in $XeF^+AsF_6^-$, Å

Xe-F(6)	2.212 (5)	[2.25][a]	As-F(3)	1.657 (6)	[1.72]
Xe-F(7)	1.873 (6)	[1.94]	As-F(4)	1.690 (5)	[1.73]
As-F(1)	1.676 (5)	[1.72]	As-F(5)	1.683 (8)	[1.74]
As-F(2)	1.690 (8)	[1.74]	As-F(6)	1.813 (6)	[1.86]

[a] Values in brackets are corrected for thermal motion according to the riding model.

Table IV. Bond Angles (deg)

F(6)-Xe-F(7)	178.9 (7)	F(2)-As-F(5)	172.7 (6)
Xe-F(6)-As	134.8 (2)	-F(6)	85.7 (5)
F(1)-As-F(2)	89.0 (4)	F(3)-As-F(4)	93.0 (4)
-F(3)	94.1 (4)	-F(5)	92.7 (5)
-F(4)	172.9 (5)	-F(6)	179.3 (7)
-F(5)	91.9 (4)	F(4)-As-F(5)	86.8 (4)
-F(6)	85.3 (3)	-F(6)	87.6 (4)
F(2)-As-F(3)	94.6 (5)	F(5)-As-F(6)	87.1 (5)
-F(4)	91.4 (5)		

Table V. Angles (deg) between Bond Vectors and Principal Axes of the Thermal Ellipsoids and Root-Mean-Square Displacements (Å)

		Angles			Rms displacements		
Atom	Vector	1	2	3	1	2	3
F(1)	F(1)-As	7	85	85	0.215	0.325	0.346
F(2)	F(2)-As	5	87	86	0.242	0.323	0.390
F(3)	F(3)-As	2	90	88	0.209	0.324	0.458
F(4)	F(4)-As	8	84	85	0.211	0.329	0.336
F(5)	F(5)-As	7	89	83	0.225	0.340	0.423
F(6)	F(6)-As	18	73	85	0.215	0.230	0.458
F(6)	F(6)-Xe	63	27	90	0.215	0.230	0.458
F(7)	F(7)-Xe	4	86	89	0.200	0.332	0.492

The $FXeFAsF_5$ unit is very similar in shape to the analogous unit in $FXeFRuF_5$[4] with which it is compared in Figure 4. In both cases the bridging fluorine is more equally shared between Xe and As(Ru) than in the corresponding $XeF_5^+MF_6^-$ compounds.[3,4]

In spite of the close similarity of molecular geometry and the fact that the arsenic and ruthenium compounds crystallize with the same space group symmetry, the unit cell shapes are dissimilar and, moreover, the molecular packing is quite different. In $FXeFAsF_5$ the long dimensions of the formula units are all nearly parallel to each other, while in $FXeFRuF_5$ there are two orientations nearly perpendicular to each other. The molecular volumes differ by less than 3%, reflecting the

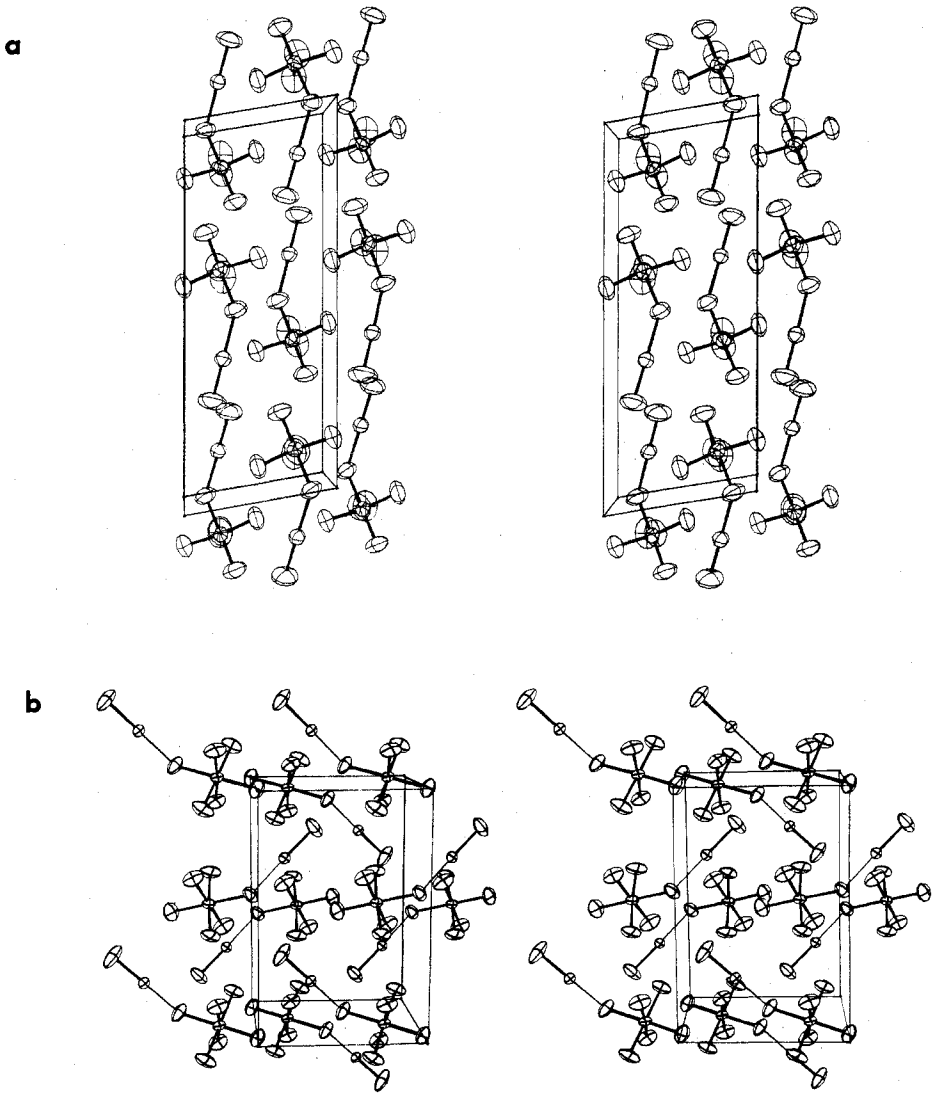

Figure 2. Stereoviews of the crystal structure (a) of $XeF^+AsF_6^-$ and (b) $XeF^+RuF_6^-$, drawn with Johnson's ORTEP.

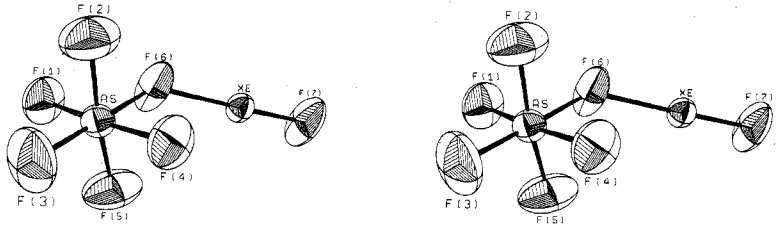

Figure 3. Stereoview of the molecular unit with 50% probability ellipsoids.

only slightly larger size of Ru compared to As, and there is little difference in the shortest intermolecular distances.

Inspection of Figure 2b reveals that in $FXeFRuF_5$ each XeF species is surrounded by a roughly cubic arrangement of RuF_6 species; the Xe···Ru distances are 3.82, 4.47, 4.54, 4.82, 4.88, 4.91, 4.99, and 5.66 Å. In $FXeFAsF_5$ (Figure 2a) each XeF species has six AsF_6 species at Xe···As distances of 3.72, 4.38, 4.44, 4.46, 4.52, and 4.80 Å. This arrangement can be viewed as a grossly distorted octahedral coordination of the cation. The next nearest arsenic neighbor of the Xe atom is at 5.84 Å. Thus to a first approximation we can represent the $FXeFRuF_5$ as developed from a CsCl (8:8 coordination) structure type whereas we can represent $FXeFAsF_5$ as derived from a NaCl type (6:6 coordination). Such representations conform with the common structure types for hexafluoroarsenates and hexafluororuthenates.[11] Thus $NO^+AsF_6^-$ is of NaCl type[12] whereas $NO^+RuF_6^-$ is of CsCl type.[13] Moreover, although the XeF_5^+ species is essentially the same in $XeF_5^+AsF_6^-$ (ref 3) and $XeF_5^+RuF_6^-$ (ref 4) the coordination is different. The coordination number differences are not to be associated with the non-transition-element–transition-element content however. Thus $NO^+SbF_6^-$ is of CsCl type[13] like $NO^+RuF_6^-$, and $XeF_5^+AuF_6^-$ has the same structure[14] as $XeF_5^+AsF_6^-$. Indeed x-ray powder photographs[15] indicate that $FXeFSbF_5$ is probably isostructural with $FXeFRuF_5$.

It appears that the difference in coordinating capability of the anions in the above structures is associated with differences in polarizability of the F ligands in the MF_6^-. In general, the CsCl type structure occurs only when at least one of the ions is highly polarizable. In those hexafluorometalates which can be unambiguously described as salts $A^+MF_6^-$, the small, less polarizable (harder) cations such as Li^+ and Na^+ generally

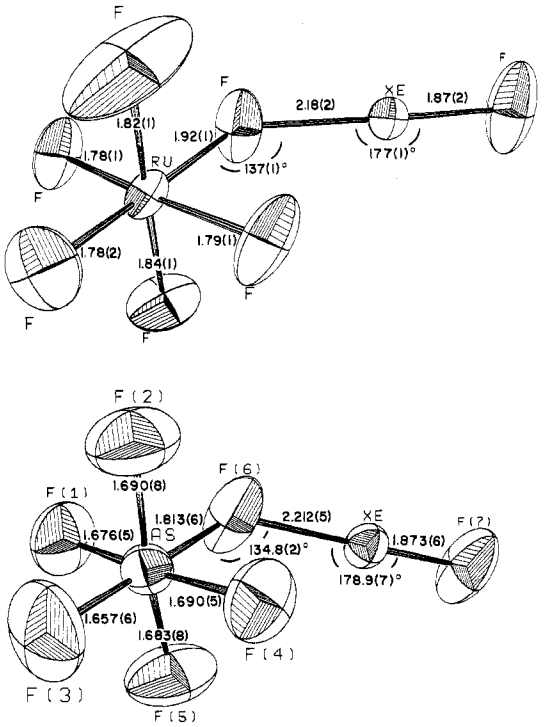

Figure 4. The formula units of $XeFAsF_6$ and $XeFRuF_6$ (ref 4), the former with 50% probability ellipsoids and the latter with 30%.

Table VI. Selected Formula Unit Volumes ($Å^3$) and Lattice Type (N = NaCl Type and C = CsCl Type) for Selected $A^+MF_6^-$ Salts

	M			
A	As	Au	Ru	Sb
Na	116.0 (N_R)[a]	?[h]	120.4 (N_R)[b]	137.0 (N)[b]
IF_6	214 (N)[c]	219 (N)[d]	?[h]	223 (C)[d,e]
Cs	138.4 (C_R)[f]	141.3 (C_R)[d]	142.6 (C_R)[b]	147.1 (C_R)[g]

[a] Reference 16. [b] Reference 11. [c] Reference 17. [d] Reference 14. [e] Reference 18. [f] Reference 19. [g] Reference 20. [h] ? indicates that the structure type is not known. Subscript R indicates a rhombohedral cell, absence indicates cubic.

prefer a NaCl type lattice, whereas the more polarizable (softer) cations, e.g., Cs^+, prefer the CsCl type. The data for selected AsF_6^-, AuF_6^-, RuF_6^-, and SbF_6^- salts,[11,14,16-20] Table VI, shows the pattern. The data indicate that the effective molecular volume of the anions increases in the sequence $AsF_6^- < AuF_6^- < RuF_6^- < SbF_6^-$. One also notes that even with a large cation such as IF_6^+, the AsF_6^- and AuF_6^- salts adopt the NaCl type lattice—presumably because the F ligands of that cation are not very polarizable (i.e., are hard). However, even with this cation, the CsCl lattice is preferred with the larger (and hence more polarizable) SbF_6^- anion.

The similarity of the $FXeFAsF_5$ and $FXeFRuF_5$ units (Figure 4) suggests that the bonding of the xenon is essentially the same for both. The bonding in XeF_2, following Coulson,[21] can be conveniently represented as a resonance hybrid of the canonical forms $(F–Xe)^+F^-$ and $F^-(Xe–F)^+$. This kind of representation permits one to make rough thermodynamic stability estimates.[22] In the $FXeFMF_5$ compounds one can represent the equivalent canonical forms as $[F–Xe]^+[F–MF_5]^-$ and $F^-[XeFMF_5]^+$. The components F^-, $[Xe–F]^+$, and $[F–AsF_5]^-$ in the listed canonical forms can each be visualized as providing each atom with its "ideal" complement of eight valence electrons.[23] The component $XeFMF_5^+$ cannot provide for this, without writing nonbonded forms such as $[(Xe–F)^+AsF_5]$ and the unrealistic $[Xe(F–AsF_5)^+]$. We therefore believe that the canonical form $F^-XeFMF_5^+$ is not important. As has been argued previously[4] we prefer to represent the formula units simply as $FXe^+MF_6^-$ and allow that the short distance between the Xe of the cation and one of the F atoms of the anion is a consequence of the cation having its positive charge centered largely at the Xe atom. This positive charge location is a consequence of the electron density in the Xe–F bond of the cation having depleted the xenon valence shell electron density (in comparison with atomic Xe). Moreover the formation of the bond in the cation must create an electron-density hole on the far side of the Xe atom (i.e., trans to the bond). One therefore anticipates that the $Xe–F^+$ species should show its highest effective positive charge when viewed along the axis toward the Xe atom. Thus the cation ought to possess a unique axis in its polarizing effects, as observed in these structures. Representation of $FXeFMF_6$ as the salts $XeF^+MF_6^-$, as for the XeF_3^+ and XeF_5^+ salts[24,4] (allowing for the polarizing effects of the cations), predicts the observed disposition of cation to anion. The model is simple and sufficient.

Acknowledgment. We thank Dr. L. K. Templeton for assistance with the absorption correction.

Registry No. $XeF^+AsF_6^-$, 26024-71-5.

Supplementary Material Available: A listing of structure factors (6 pages). Ordering information is given on any current masthead page.

References and Notes

(1) Work supported by the U.S. Energy Research and Development Administration.
(2) F. O. Sladky, P. A. Bulliner, and N. Bartlett, *J. Chem. Soc. A*, 2179 (1969).
(3) N. Bartlett, B. G. DeBoer, F. J. Hollander, F. O. Sladky, D. H. Templeton, and A. Zalkin, *Inorg. Chem.*, **13**, 780 (1974).
(4) N. Bartlett, M. Gennis, D. D. Gibler, B. K. Morrell, and A. Zalkin, *Inorg. Chem.*, **12**, 1717 (1973).
(5) J. Binenboym, H. Selig, and J. Shamir, *J. Inorg. Nucl. Chem.*, **30**, 2863 (1968).
(6) S. M. Williamson, *Inorg. Synth.*, **11**, 147 (1968).
(7) L. K. Templeton and D. H. Templeton, Abstracts, American Crystallographic Association Proceedings, Series 2, Vol. 1, 1973, p 143.
(8) P. A. Doyle and P. S. Turner, *Acta Crystallogr., Sect. A*, **24**, 390 (1968).
(9) D. T. Cromer and D. Liberman, *J. Chem. Phys.*, **53**, 1891 (1970).
(10) The first crystals of $FXeFAsF_5$ were grown from a sample mislabeled as $(FXe)_2SO_3F^+AsF_6^-$. Single crystals of this compound have not yet been obtained.
(11) D. Babel, *Struct. Bonding (Berlin)*, **3**, 1 (1967).
(12) N. K. Jha and N. Bartlett, to be submitted for publication.
(13) N. Bartlett and D. H. Lohmann, *J. Chem. Soc.*, 5253 (1962).
(14) N. Bartlett and K. Leary, *Rev. Chim. Minér.*, **13**, 82 (1976).
(15) R. Mews, unpublished observation.
(16) L. E. Levchuk, B.Sc. Thesis, University of British Columbia, April 1963.
(17) S. P. Beaton, Ph.D. Thesis, University of British Columbia, 1966; K. O. Christe and W. Sawodny, *Inorg. Chem.*, **6**, 1783 (1967).
(18) F. A. Hohorst, L. Stein, and E. Gebert, *Inorg. Chem.*, **14**, 2233 (1975).
(19) B. Cox, *J. Chem. Soc.*, 876 (1956).
(20) N. Schoewelius, *Ark. Kemi Mineral. Geol.*, **B16**, No. 7 (1942).
(21) C. A. Coulson, *J. Chem. Soc.*, 1442 (1964).
(22) M. Wechsberg, P. A. Bulliner, F. O. Sladky, R. Mews, and N. Bartlett, *Inorg. Chem.*, **11**, 3063 (1972).
(23) We can represent arsenic in AsF_6^- as achieving an octet by writing canonical forms in which the arsenic atom makes electron-pair bonds to two F ligands and four single-electron bonds to the remaining four F ligands. A resonance hybrid of such canonical forms is equivalent, in describing the net F–As bonding, to a molecular orbital description (for the octahedral group) which provides filled bonding orbitals A_{1g}^2 and T_{1u}^6 and filled nonbonding orbitals E_g^4.
(24) D. E. McKee, A. Zalkin, and N. Bartlett, *Inorg. Chem.*, **12**, 1713 (1973).